The EUMETSAT Network of Satellite Application Facilities

NWP SAF
Numerical Weather Prediction

Visiting Scientist mission report

Document NWPSAF-MO-VS-046

Version 1.0
21 February 2012

TELSEM 1D-var experiments at the Met Office: final report

Filipe Aires, Sreerekha Thonipparambil, Catherine Prigent and Roger Saunders

Met Office

ECMWF

Royal Netherlands Meteorological Institute
Ministry of Transport, Public Works and Water Management

METEO FRANCE
Toujours un temps d'avance

This documentation was developed within the context of the EUMETSAT Satellite Application Facility on Numerical Weather Prediction (NWP SAF), under the Cooperation Agreement dated 1 December, 2006, between EUMETSAT and the Met Office, UK. The partners in the NWP SAF are the Met Office, ECMWF, KNMI and Météo France.

Change record			
Version	Date	Author / changed by	Remarks
1.0	21.2.12	F.Aires	

TELSEM 1D-var experiments at MetOffice

Final report

Prepared by:

Filipe Aires,
Sreerekha Thonipparambil,
Catherine Prigent,
and Roger Saunders

February 21, 2012

Abstract

TELSEM is a microwave land surface emissivity interpolator recently developed in the NWP SAF. It is anchored to a long SSM/I climatology of emissivities but allows to estimate microwave emissivities for other present or future instruments. The objective of this study is to estimate the potential impact of TELSEM in a NWP operational context. 1D-var experiments are conducted over clear situations, for AMSU-A instrument, over land. They illustrate that TELSEM increases very significantly the quality of background information in NWP systems and that it increases by about one third the number of satellite microwave observations that can be exploited by NWP centres over land .

Chapter 1

Description of the experiment

1.1 Motivation

In order to help the assimilation of microwave radiances over land, a land surface microwave emissivity interpolator for RTTOV has recently been completed as an NWP SAF associate scientist (AS) mission (Aires *et al.*, 2009). TELSEM (Tool to Estimate Land Surface Emissivity in the Microwave) is based on a parameterization anchored to a SSM/I emissivity atlas (Prigent *et al.*, 2008). It was demonstrated to provide improved simulations of microwave radiances over land for ASMR-E, AMSU-A, HSB and MHS (Aires *et al.*, 2011). Furthermore, it has been shown that TELSEM provides a good first approximation of the emissivity that can be further refined by retrieval algorithms: statistical (Aires *et al.*, 2001; 2011), physical, variational (Karbou *et al.*, 2006), assimilation. As planned in the original AS mission, it is desirable to test TELSEM in an NWP context and quantify its impact. The MetOffice already had a framework for testing changes to the land surface emissivity and so was ideally placed to provide the infrastructure for this work.

TELSEM is anchored to a SSM/I emissivity atlas. In order to analyze the capacity of TELSEM to produce pertinent information for other instruments, we will evaluate its emissivity estimates at AMSU-A frequencies (See Table 1.1 and Figure 1.1). Comparison with direct estimates of the AMSU-A emissivities will be done when appropriate.

1.2 Experimental conditions for the 1D-var

1D-var Experiment - Various options have been considered based on (1) the timeframe for this project, (2) the availability of already existing tools, and (3) the flexibility of the MetOffice framework. It has been decided that the OPS

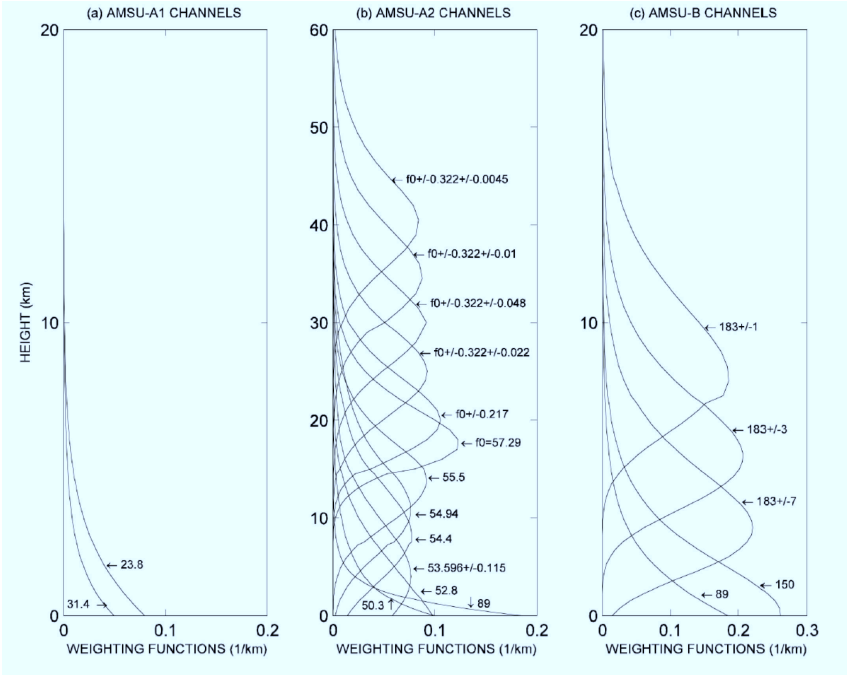

Figure 1.1: AMSU-A and -B weighting functions for a US standard tropical atmosphere (WV=42 kg/m^2) at nadir, assuming a surface temperature of 299 K and a surface emissivity of 0.95 for: (a) AMSU-A1, (b) AMSU-A2, and (c) AMSU-B channels.

Channel number	Frequencies in GHz	Noise in K
1	23.8	0.30
2	31.4	0.30
3	50.3	0.40
4	52.8	0.25
5	53.596±0.115	0.25
6	54.4	0.25
7	54.94	0.25
8	55.5	0.25
9	57.290344 (= F_{LO})	0.25
10	F_{LO}±0.217	0.40
11	F_{LO}±0.3222±0.048	0.40
12	F_{LO}±0.3222±0.022	0.60
13	F_{LO}±0.3222±0.010	0.80
14	F_{LO}±0.3222±0.0045	1.20
15	89.0	0.50

Table 1.1: Instrument characteristics for AMSU-A onboard MetOp, a cross-track instrument with 48 km spatial resolution at nadir.

system is not flexible enough at this stage for assimilation experiments. The introduction of more data and the way we would have to take into account incidence angles and uncertainty covariance matrices would be too complex and time-consuming to be implemented in the timeframe of this project. As a consequence, it has been decided that no assimilation experiments would be conducted, only 1D-var experiments are performed in this study. The 1D-var system of MetOffice is run on real conditions, the usual geophysical parameters are retrieved (temperature, water vapour, surface temperature, etc.), together with the emissivity at 23, 31, 50.3 and 89 GHz.

Clear sky - It has been shown that using microwave surface emissivities has a strong positive impact for atmospheric profile retrievals under cloudy conditions (Aires *et al.*, 2010; Aires *et al.*, 2011; Bernardo *et al.*, 2012). TELSEM is also used in the precipitation retrieval algorithm of GPM (Global Precipitation Mission) (Ferraro *et al.*, 2012). Activity also exist at ECMWF in order to use land surface microwave emissivities for the assimilation of cloudy or precipitating observations (e.g., O'Dell, C. and P. Bauer, 2007). In this study, the goal is to assess the ability of TELSEM to estimate reliable emissivity first guesses for an independent instrument (i.e., AMSU-A), in an operational context, independently of the difficult problem of retrievals in cloudy or precipitating conditions. Only clear situations are considered here.

Cloud detection - The cloud detection approach used at the moment for lower troposphere channels over land is based on a simple filter (Karbou *et al.*, 2010): the situation is considered to be cloudy when $(O - B) > 0.7$ K for channel 4 (52.8 GHz) (See weighting function in Figure 1.1). It should be noted that more sophisticated microwave cloud filtering could be used (Aires *et al.*, 2011a) but

this would be the subject of a future study. If the sitation is flaged as cloudy, then channels 1, 2, 3, 4, 5 and 15 of AMSU-A are not used in the 1D-var scheme. The 1D-var is performed for the other channels, but since the window channels are not considered anymore in this case, they are of no interest here and we will exclude these situations from our statistics. It should be noted that the cloud flag $(O - B) < 0.7\ K$ for channel 4 is very limitating: only situations with a very good background would be classified to be clear, which biases the statistics. This topic will be discussed later.

Database - The OPS system has been used to extract files including the inputs for the 1D-var and the real observations from AMSU-A instrument on board METOP platform. Some auxiliary information is also kept in order to diagnoze the results. Furthermore, the profiles and BT simulations after convergence of the 1D-var are also kept (only for situations that have converged). Two days have been extracted in order to sample the seasonal variability: January 15^{th} and July 15^{th} of 2008. Four cycles of 6 hours are considered for each day, which should allow diurnal cycle sensitivity assessment (e.g. cycle 00 corresponds to the satellite data that is included between 9PM and 3AM, cycle 06 includes data between 3AM and 9AM, etc.). It will be seen in the following that the use of much more days would be extremely valuable for the analysis since the results appear to be dependant on the day. However, given the time constraints, w limited our study to these two days.

Microwave emissivity - The "Atlas builder" generating the emissivities from TELSEM (chapter 2.1) has been used to add AMSU-A emissivities to the background, B, before the 1D-var experiment. TELSEM is used in the online mode, i.e. the emissivity is computed for each data point in the OPS outputs. In this way, the emissivity background from TELSEM uses the polarization of channels and the incidence angle. TELSEM will provide an emissivity estimate for all AMSU-A channels but only channels 23, 31, 50.3 and 89 GHz will be retrieved. The TELSEM emissivities will be compared in our experiments to a "Fixed" emissivity at 0.95. In some cases, the results will also be compared to a direct estimation of the emissivity using AMSU-A observations (2007 estimations by Karbou), called AMSU-A-derived in this study.

Spatial resolution - The spatial resolution of the emissivity information from TELSEM needs to be as close as possible to the satellite observations. As a consequence, the Fortran code generating the emissivities uses the nominal TELSEM resolution: a $0.25° \times 0.25°$ equal-area grid and, in the code, the closest TELSEM pixel will be used for each data point (routine emis_interp_ind_mult in the TELSEM package). Furthermore, it should be noted that the link between surface temperature and emissivity is very important for surface-sensitive channels. TELSEM will be used with a good spatial resolution but the surface temperature comes from the model and this discrepancy in spatial resolution can be source of difficulties due this discrepancy on the spatial resolution.

Uncertainty covariance matrices - The emissivity uncertainty used in the 1D-var is based in this study on the emissivity variability in the global monthly atlas. This is a crude estimation of course. However, the 1D-var system at MetOffice is set-up to run with a unique covariance matrix of the emissivity uncertainty, the

previous 1D-var experiment at MetOffice did not include any better uncertainty information on emissivities. Unfortunatly, it seems too complex to change it at this stage in the MetOffice system. This is a strong limitation of our 1D-var experiment because the estimation of emissivity uncertainty is a key feature of TELSEM and we will not be able to test it here.

Diagnostics - Various diagnostic tools can be used to assess the quality of the emissivity information:

- $(O - B)$, where O are the satellite observations, and B are the brigthness temperatures simulated with the background profiles;
- $(O - R)$, where R are the brightness temperatures simulated with the retrieved quantities;
- The number of situations that have converged in the 1D-var is also a good diagnostic for the quality of the emissivity information.

Chapter 2

TELSEM

2.1 Atlas builder

A Fortran code called METOFFICE_atlas.f90 has been delivered to MetOffice. This code uses the TELSEM interpolator to build emissivity atlases. The code has been developed to estimate AMSU-A and MHS emissivities at various incidence angles, for various months of the year. Since TELSEM provides emissivities and covariance matrices for both vertical and horizontal polarizations, the mixing of the polarizations for each channel had to be implemented. This involves some matrix manipulations, especially for the covariance matrix.

An IDL code to represent the resulting emissivities and uncertainties has been developed and delivered at MetOffice. It uses the SAT_MAP library.

The code has been used to create the AMSU-A and MHS (20 channels) emissivity atlas (Figure 2.1) for the twelve months of the year. Five scan-angles have been considered: 5, 15, 25, 35, and 45° (see Figure 2.1 for emissivity at 5 and 45°). The atlas also includes the standard deviation of each of the 20 channels (the full covariance matrix has not been included so far in the 1D-var experiment but TELSEM provides this information easily). It should be noted that in the 1D-var experiment presented in the following section, these atlases will not be used directly: since the exact incidence angle is provided for each data point, the direct use of the code estimates specific emissivities for each satellite observation.

2.2 Surface classification

A surface classification is used by TELSEM. We use in the following this classification to analyze the results of the 1D-var experiments.

The surface classification is based on a SSM/I-derived emissivity climatology over 8 years (1993-2000). The NSIDC information is used to separate snow and ice pixels, and our surface water climatology (Prigent *et al.*, 2006) filters out the surface waters. The resulting classification in self-similar surfaces is presented

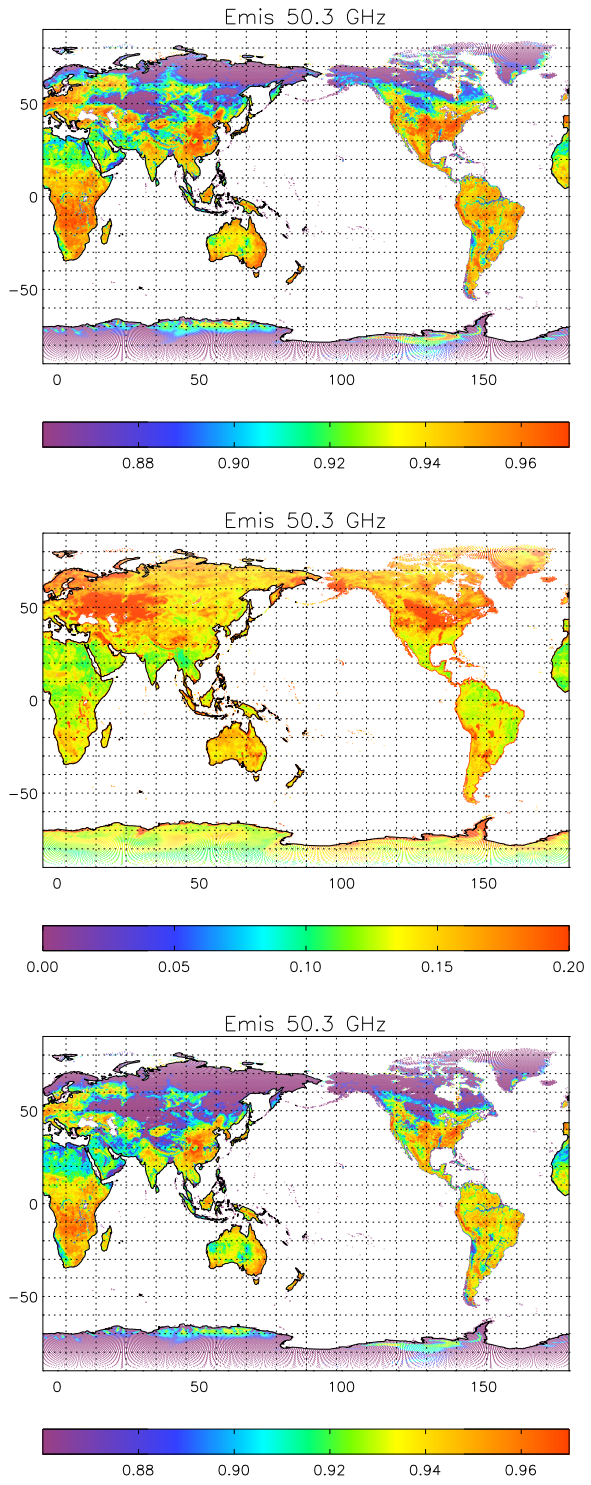

Figure 2.1: TELSEM emissivity at 50.3 GHz at 5° incidence angle (top), corresponding uncertainty estimates (middle), and emissivity at 50.3 GHz at 45° incidence angle (bottom), for January.

in 2.2, for January and July. In this example, classes 1 to 5 correspond to decreasing vegetation density. Classes 6-9 are for snow/ice-covered pixels. Class 10 represents pixels with surface water. Note that due to the large variability of the snow emissivities, several classes are necessary to represent the snow regions.

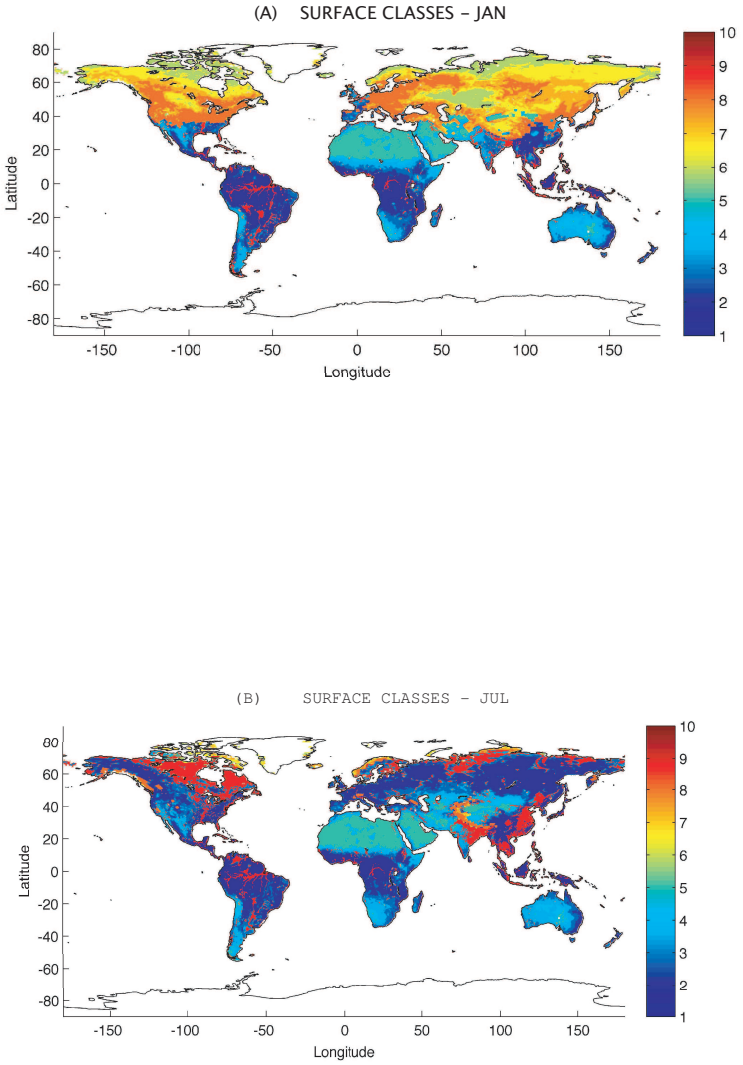

Figure 2.2: Surface classification using microwave emissivity information for (A) January and (B) July.

Chapter 3

1D-var results

3.1 Inputs

The inputs of the 1D-var are the analysis of the MetOffice for surface properties and atmospheric profiles (e.g., temperature or water vapour). The only differences between our three configurations come from the introduction of different microwave emissivities. In Figure 3.1, the surface temperature and the surface emissivity at 21.8 GHz are illustrated for three configurations: Fixed emissivity at 0.95, TELSEM and AMSU-A-derived emissivities. It can be seen that we have used the angle dependency of the emissivities for TELSEM. Furthermore, the major differences appear at high latitudes.

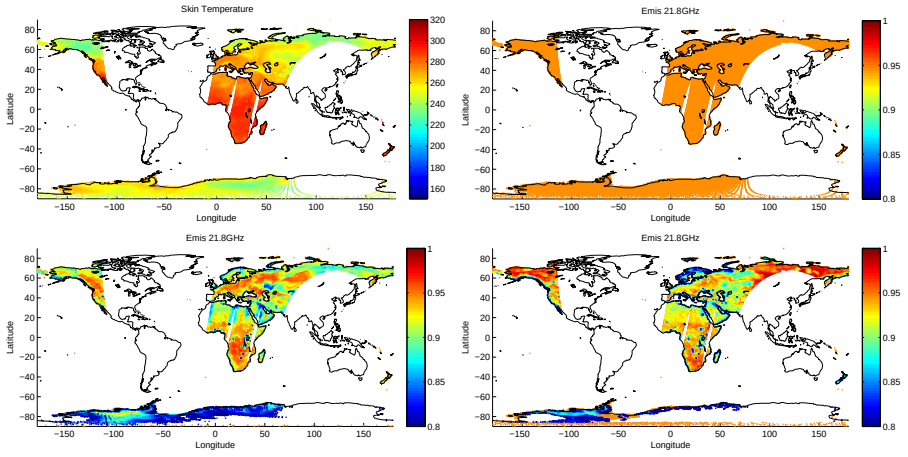

Figure 3.1: Inputs for the 1D-var, from top to bottom: Ts, emissivity at 21.8 GHz for Fixed, TELSEM and AMSU-A-derived, for January 15^{th}, at cycle 00:00AM.

Figure 3.2 represents the emissivities at 21.8 GHz and 89 GHz for AMSU-A-derived retrievals (from Karbou) and from TELSEM over South America. Again, it can be noted the angle dependency appears for TELSEM. Hydrological structures around the Amazon or the Orinoco appear very clearly on the TELSEM estimate. The salar in Bolivia are also well delineated.

3.2 Radiative transfer simulations on the background

In this section, we analyze the brightness temperatures simulated by RTTOV when using the background information (See section 3.1). The differences between O, the real Observations, and B, the brightness temperatures corresponding to the Background state, is probably the more direct way to monitor the quality of the various emissivity sources because after the 1D-var, it is difficult to say if an emissivity is better or not since all the geophysical parameters can change during the retrieval.

3.2.1 $(O - B)$ statistics - No filtering

In this section, $(O - B)$ statistics are presented without any cloud filtering. All surface classes and scanning angles are condidered in the statistics. In Figure 3.3, the histograms of $(O - B)$ are represented for each AMSU-A channels. The bias and RMS errors are also indicated in the figure. The statistics are provided for Fixed (red), AMSU-A-derived (blue) and TELSEM (green) emissivities. Both AMSU-A-derived and TELSEM provide a strong improvement as compared to the Fixed emissivity configuration. AMSU-A-derived and TELSEM statistics are not very different in terms of RMS. However, it should be noted that bias is higher for TELSEM than for AMSU-A-derived. This stronger biases are compensated by TELSEM by a lower standard deviation of the errors which results in a comparable RMS errors. We can explain this behavior by the fact that the SSM/I emissivities used to calibrate TELSEM have been estimated using Ts estimates from infrared satellite observations (from ISCCP). It is well-known that the surface temperatures are often questionable in NWP outputs, expecially over arid regions. This would explained the bias in TELSEM emissivities. The lower STD errors of TELSEM seem to compensate well these biases. The higher STD errors in AMSU-A-derived can result from cloud contamination or a limited number of observations to compute the atlas (due to the scanning geometry).

3.2.2 $(O - B)$ statistics - Cloud and 1D-var filtering

In this section, contrarily to 3.3, the cloud filtering is used, and only data for which the 1D-var has converged are kept in the statistics. Furthermore, in order to perform these statistics on the same ensemble for the three configurations, only the common situations that have converged are used here (otherwise, we

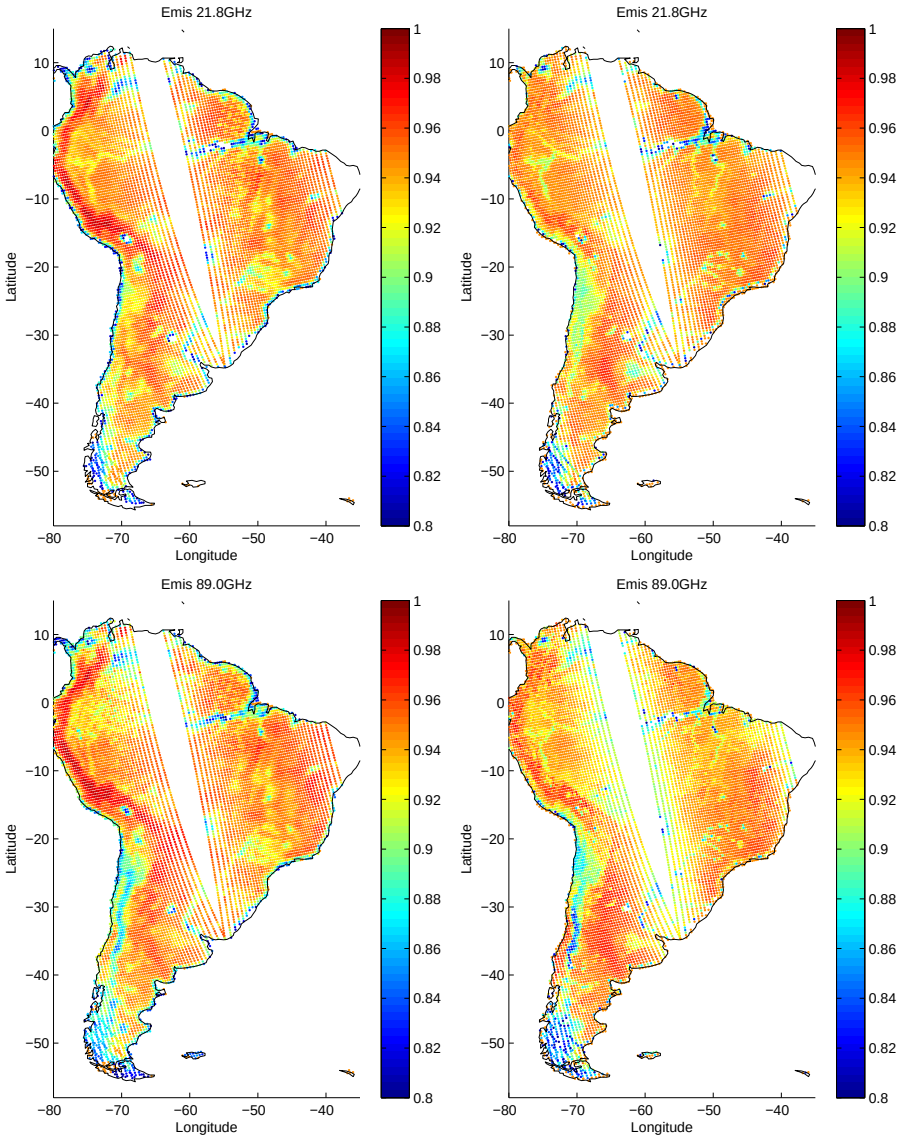

Figure 3.2: Emissivities at 21.8 GHz (upper part) and 89 GHz (lower part) for AMSU-A-derived retrievals (from Karbou, left panel) and from TELSEM (right panel), for July 15^{th}, at cycle 18.

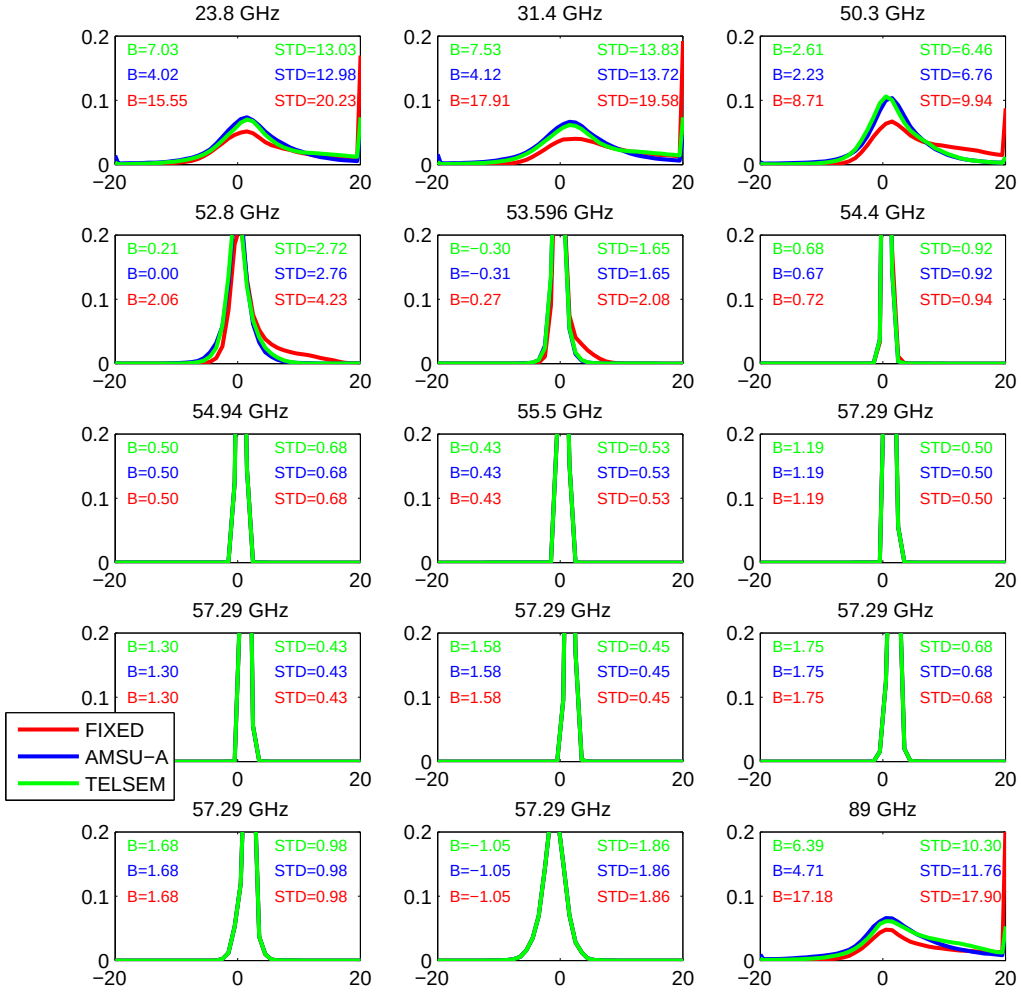

Figure 3.3: Statistics for $(O - B)$ for all AMSU-A channels, for Fixed (red), AMSU-A-derived (blue) and TELSEM (green) emissivities. These statistics are for two days in January and July 2008, and all surface classes. No cloud filtering is used. Bias and RMS statistics are provided.

would compare statistics on different ensembles). In Figure 3.4, the histograms of $(O-B)$ are represented for channels 23.8, 31.4, 50.3, 52.8, 57.29 and 89 GHz. The bias and RMS errors are also indicated in the figure. The statistics are provided for Fixed (black), AMSU-A-derived (green) and TELSEM (red) emissivities. Differences are not very important but this is expected since these statistics show only results for "easy" situations, where even the fixed emissivity has converged.

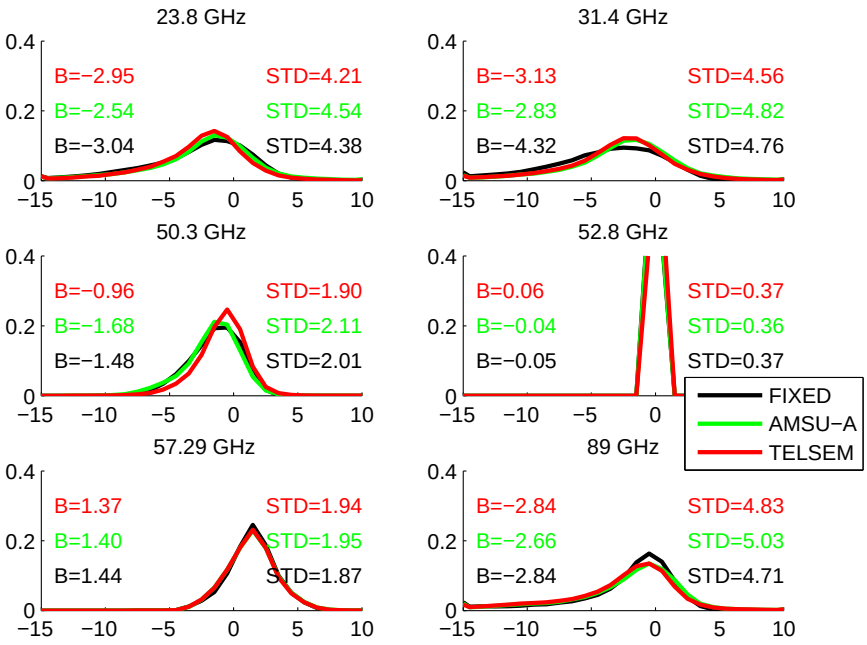

Figure 3.4: Statistics for $(O-B)$ for fixed (black), AMSU-A-derived (green) and TELSEM (red) emissivities. These statistics are for the situations that have converged for the three emissivity sources, for two days in January and July 2008, and all surface classes. Bias and RMS statistics are provided. A cloud-flag has been used to keep only clear cases.

It can be seen that the fixed emissivity seems to be biased compared to TELSEM or AMSU-A-derived emissivities. TELSEM and AMSU-A-derived seem to be a noticable improvement for channel 31.4 GHz, and TELSEM seems to be better for channel 50.3. For sounding channels, no difference can be seen between the three different sources of emissivities, as expected.

3.3 1D-var

In this section, only situations for which the 1D-var has converged (and that are potentially assimilated in a NWP system) are considered. It is important to note that it is difficult to assess precisely the contribution of the quality of the emissivity in the statistics since all the geophysical parameters (surface and atmospheric) are changed during the 1D-var.

3.3.1 $(O-R)$ statistics - Cloud and 1D-var filtering

Figure 3.5 is similar to Figure 3.4 but this time, the real satellite observations, O are compared to R, the brightness temperatures associated to the retrievals. The major improvement from TELSEM is for channel 31.4 GHz. For other

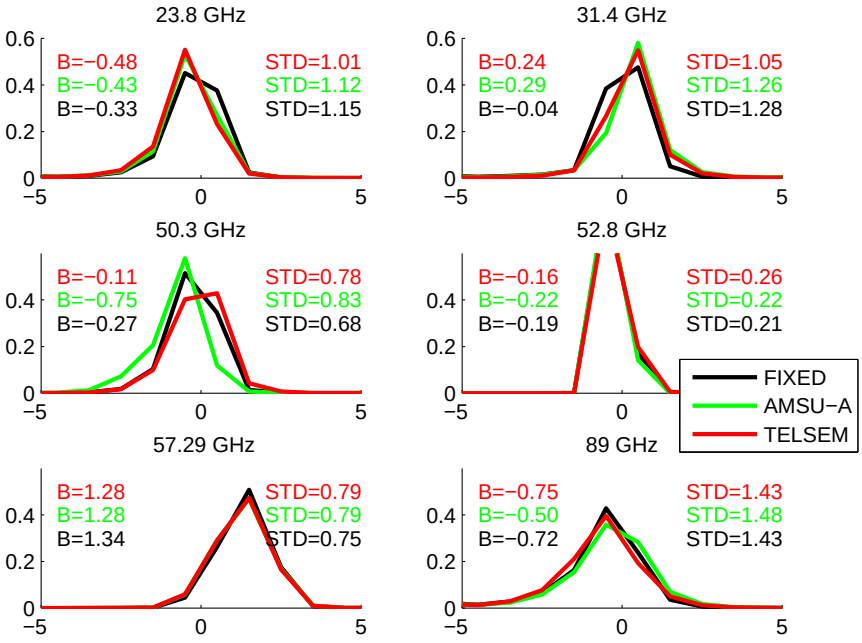

Figure 3.5: Statistics for $(O-R)$ for fixed (black), AMSU-A-derived (green) and TELSEM (red) emissivities. This statistics is for the points that have converged for the three emissivity sources, for two days in Janyaru and July 2008, and all surface classes.

channels, TELSEM results are quite close to the fixed emissivity. This shows that the statistics on the points that have converged for the three emissivity sources should be considered with caution. Since the 1D-var has converged for

all these three emissivity sources, it means that the emissivities from TELSEM and AMSU-A-derived are both close to the fixed one.

3.3.2 Sensitivity to surface class

Figure 3.6 represents the number and percentage of situations that have converged in the 1D-var for Fixed and TELSEM emissivities. The percentages include the cloud filtering, more than half of the rejections are the result of this cloud filtering (See section 1.2). The statistics have been done using the two days, in January and July. TELSEM appears to be very interesting for snow-ice classes (i.e. classes 6, 7 and 8). TELSEM represents an important improvement too for class 10 that gathers surfaces with surface water. TELSEM is overall an improvement for all classes except for classes 3, 4 and 5 (i.e. arid regions). However, these results need to be further analyzed, the results have a significant variation from one day to another and more OPS data would be necessary to obtain stable statistics.

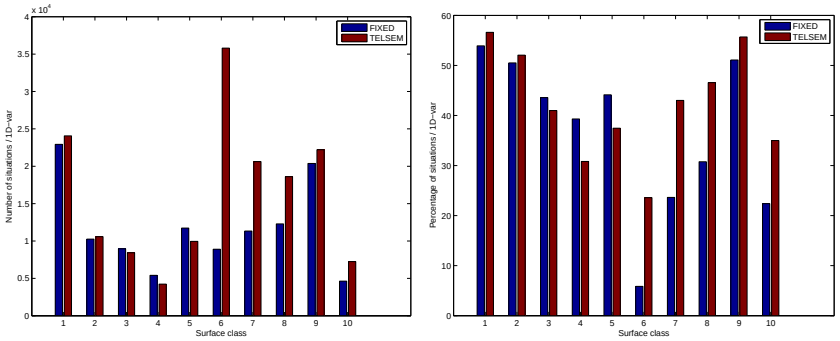

Figure 3.6: Number (left) and percentage (right) of situations that have converged in the 1D-var for Fixed and TELSEM emissivities by surface class (Section 2.2).

The reason for lower 1D-var convergence for TELSEM in arid regions could be explained by the fact that TELSEM emissivities have been calculated using surface temperature from IR satellite observations (ISCCP). It has been shown that satellite surface temperatures and Ts analysis from NWP centers can differ significantly (see e.g. *Paul et al.*, 2012). So the degraded results for arid regions (i.e. where Ts error are the most important) could result from an incompatible surface temperature, not from an error in the emissivity estimate.

3.3.3 Sensitivity to scanning angle

Figure 3.7 shows the scanning angle dependency of the number of points that have converged through the 1D-var. The percentage of situations is also provided (again, this percentage also includes the cloud filtering). It is surprising

to note that, while when using the Fixed emissivity, the percentages are very close for all scanning angles, the percentages increase with angle for TELSEM. Further analysis would be necessary to explain this behavior. However, it should

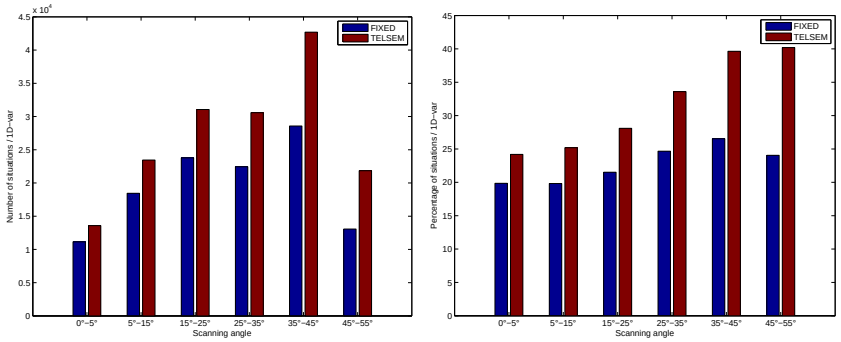

Figure 3.7: Number (left) and percentage (right) of situations that have converged in the 1D-var for Fixed and TELSEM emissivities by scanning angle.

be noted that scanning angle is an important factor. Some tests have been conducted with TELSEM with no angle dependency (not shown) and the impact on results was significant.

3.3.4 Sensitivity to the data day

Figure 3.8 represents the percentage of points for which the 1D-var converges. These statistics are provided for the Fixed and TELSEM emissivity configurations, for January and July, each time for cycle 00, 06, 12 and 18. It can be seen

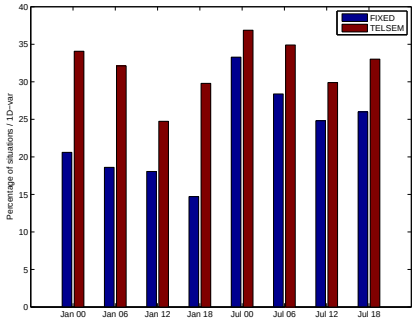

Figure 3.8: Percentage of of situations that have converged in the 1D-var for Fixed and TELSEM emissivities for the two days and four cycles.

that results are much better for January than for July. One possible explanation is that greater improvement in January is related to the better representation

f snow emissivity overh the northern latitudes. In summer, smaller benefit can be obtained. However, this sensitivity of the statistics to the data day would required to be analyzed for a larger dataset.

3.3.5 Comparison with direct emissivity estimates

TELSEM is designed to provide a first guess in emissivity for a large set of instruments because it can interpolate its emissivity estimates on frequency, incidence angle or polarization conditions. This first guess can then be used by a retrieval algorithm that will refine it. Various retrieval techniques can be used for this task: statistical retrieval algorithms (Aires *et al.*, 2001; Aires *et al.*, 2012; Bernardo *et al*, 2012), or assimilation (Karbou *et al.*, 2006).

However, the methodology developed in (Prigent *et al.*, 2006) can be used to estimate directly the emissivity from the satellite observations and some *a priori*, i.e., mainly the water vapour profile, surface temperature and cloud flag (Prigent *et al.* 1997; Karbou *et al.*, 2005). Since TELSEM is a very general parameterization of the emissivity, the direct estimation of the emissivities should always be more precise.

A previous experiment has been conducted some time ago at MetOffice to use direct estimates of the AMSU-A-derived emissivity. This experiment used the estimates from Karbou, i.e. same emissivity retrieval algorithm as Prigent *et al.* (2006). We have compared the number of situations that have converged through the 1D-var when using the three emissivity configurations, and it confirms that the direct estimation from the satellite observations is overall slightly better: the number of situations that have converged is 117456 (26.5%) for the Fixed emissivities, 163191 (36.8%) for the TELSEM emissivities and 176059 (39.7%) for the AMSU-A-derived emissivities. Note that some points in the AMSU-A-derived emissivity atlas are missing (about 20.000 thousands for an overall dataset of 500.000 situations). The radiative transfer simulations on these points appear to be questionable. These points have to be suppressed in our $(O - B)$ statistics. They are automatically suppressed by the "cloud filtering" $(O - B) > 0.7$ K based on channel 4.

Chapter 4

Conclusion and perspectives

4.1 Conclusion

In this study, the impact of TELSEM for 1D-var experiments has been tested in an NWP context. The use of TELSEM increases strongly the quality of the background state for the microwave surface-sensitive channels. It was shown that compared to a constant microwave emissivity, the use of TELSEM increases by almost a third the number of situations that converge in the 1D-var algorithm.

TELSEM is a tool that is able to provide a first guess information in emissivity for a large variety of cross-track or conical microwave instruments. It is anchored to a SSMI/I microwave atlas derived from a long climatology (Prigent *et al.*, 2006). When tested on a specific instrument, TELSEM is almost as good as a direct estimation of the emissivity, at a much lower development cost. Furthermore, compared to a fixed atlas, TELSEM includes an angle dependency, frequency and polarization interpolation, and uncertainty characterization, with a flexibility in spatial resolution.

In this study, it was also pointed out that it is difficult to disantangle, in such 1D-var experiments, the contribution of the surface temperature and emissivity. An error on the surface temperature can be compensated by an opposite error for the emissivity. Therefore, it is difficult to validate the surface emissivity without a validation of the surface temperature (see Paul *et al.*, 2012 for such a validation in the IR domain). TELSEM uses surface temperatures from IR satellite observations (i.e. ISCCP dataset) that are and probably less "compatible" with surface temperatures from NWP centers, but probably closer to the actual truth. In particular, it is known that the surface temperature in operational analyses are limited (e.g. bias in particular in the arid regions), which can explain the fact that TELSEM seems to have less impact for these regions.

4.2 Perspectives

We have pointed out in this report some practical limitations in the experiment that we have conducted at MetOffice. The first perspectives would be to alleviate these limitations, namely:

- Increase the number of situations in our analysis;
- Use the uncertainty covariance matrix on TELSEM emissivities in the 1D-var;
- Improve the cloud flag that is presently questionable.

Other perspectives would be to validate the emissivities that are retrived by the 1D-var by validating the surface temperatures that are obtained. It is important to disantangle the contribution of the surface temperature and emissivity in this type of problem. The other important perspective would be to perform assimilation and measure the impact of TELSEM on the forecast errors. We could also test TELSEM for other instruments, in particular using SSMI/S on board the DMSP platforms (it would be interesting to measure the impact of TELSEM for a conical instrument). It has been shown that TELSEM is beneficial for cloudy retrievals too, so our experiment could be extended for the assimilation of cloudy and precipitating situations.

Acknowledgements

We would like to thank the Eumetsat NWP SAF (Satellite Application Facility) and in particular Brian Conway for financing this study. We thank also James Hocking from the Met Office for interesting discussions about the implementation of TELSEM in RTTOV. We would like to thank Steve English who has initiated this work with Sreerekha Thonipparambil at MetOffice some time ago.

Bibliography

Aires, F., C. Prigent, W.B. Rossow, and M. Rothstein, A new neural network approach including first-guess for retrieval of atmospheric water vapor, cloud liquid water path, surface temperature and emissivities over land from satellite microwave observations, *J. of the Geophys. Res.*, Vol. 106, No. D14, pp. 14,887-14,907, July 27, 2001.

Aires, F., Prigent, C. and F. Bernardo, TELSEM: a tool to estimate land surfac emissivities at microwave frequencies, Eumetsat-NWP SAF report, November 2009.

Aires, F., F. Bernardo, H. Brogniez, and C. Prigent, An Innovative Calibration Method for the Inversion of Satellite Observations, *J. Appl. Meteorol. Climatol.*, 49, 12, 2458-2473, december 2010.

Aires, F., Marquisseau, F., Prigent, C., and Seze, G., A land and ocean microwave cloud classification derived from AMSU-A and -B, calibrated on MSG-SEVIRI infrared and visible observations, *Month. Weat. Rev.*, , 139, 2347-2366, doi: http://dx/doi.org/10.1175/MWR-D-10-05012.1, 2011a.

Aires, F., C. Prigent, F. Bernardo, C. Jiménez, R. Saunders, P. Brunel, A Tool to Estimate Land Surface Emissivities at Microwaves (TELSEM) frequencies for use in numerical weather prediction, *Q. J. R. Meteorol. Soc.*, in press, 2011b.

English, S.J., The importance of accurate skin temperature in assimilating radiances from satellite sounding instruments, *IEEE Trans. Geosci. Remote Sens.*, 46, pp. 403-408, 2008.

Eyre, J.R. (1991), A fast radiative transfer model for satellite sounding systems, ECMWF Research Dept. Tech. Memo. 176 (available from the librarian at ECMWF).

Karbou, F., F. Aires, C. Prigent, and L. Eymard, Potential of AMSU-A and -B measurements for atmospheric temperature and humidity profiling over land, *J. of the Geophys. Res.*, *110*, D97109, doi: 10.1029/2004JD005318, 2005.

Karbou, F., E. Gerard, and F. Rabier, Microwave land emissivity and skin temperature for AMSU-1 and -B assimilation over land, QJRMS, 132, 620, pp. 2333-2355, 2006.

Karbou, F., E. Grard, F. Rabier Global 4D-Var assimilation and forecast experiments using AMSU observations over land. Part-I : Impact of various land surface emissivity parameterizations, Weather and Forecasting, 25, 5-19, doi : 10.1175/2009WAF2222243.1, 2010.

O'Dell, C. and P. Bauer, Assimilation of precipitation-affected SSMIS radiances over land in the ECMWF data assimilation system, ECMWF report, 2007.

Prigent C., W.B. Rossow, and E. Matthews, Microwave land surface emissivities estimated from SSM/I observations, *J. of the Geophys. Res.*, *102*, 21867-21890, 1997.

Prigent, C., F. Aires, and W.B. Rossow, Land surface microwave emissivities over the globe for a decade, *Bull. of the Amer. Meteorol. Soc.*, DOI:10.1175/BAMS-87-11-1573, 1572-1584, 2006.

Prigent, C., E. Jaumouille, F. Chevallier, and F. Aires, A parameterization of the microwave land surface emissivity between 19 and 100 GHz, anchored to satellite-derived estimates, *IEEE Trans. Geosci. Remote Sens.*, 46, 344-352, 2008.

Saunders, R.W., M. Matricardi, and P. Brunel (1999), An improved fast radiative transfer model for assimilation of satellite radiance observations, *Q. J. R. Meteorol. Soc.*, *125*, pp. 1407–1425.

Ferraro, R., C. Peters-Lidard, C. Hernandez, F.J. Turk, F. Aires, C. Prigent, W. Lon, S-A. Boukabara, F. Furuzawa, K. Gopalan, K. Harrison, F. Karbou, L. Li, C. Liu, H. Masunaga, L. Moy, S. Ringerud, G. Skofronick-Jackson, Y. Tian, N-Y. Wang, An evaluation of microwave land surface emissivities over the continental UnitedStates to benefit GPM-era precipitation algorithms., *IEEE Trans. Geosci. Remote Sens.*, , submitted, 2012.